RSC Advances

PAPER

View Article Online
View Journal | View Issue

Cite this: *RSC Adv.*, 2022, **12**, 31442

Enhancing magnetic coupling through protonation of benzylideneaniline-bridged diradicals and comparison with stilbene- and azobenzene-based diradicals†

Fengying Zhang, *[a] Yiwei Feng,[b] Xinyu Song [b] and Yuxiang Bu [b]

Taking nitroxide radicals as spin sources, we explore the intramolecular magnetic coupling interactions of the *trans*- and *cis*-forms of benzylideneaniline (BA)-bridged diradicals, in which the central –CH=N– unit can undergo single protonation to convert to its protonated counterpart or *vice versa*. The calculated results for these two pairs of diradicals (protonated *versus* unprotonated *trans* and *cis* forms) verify that the signs of their magnetic coupling constants *J* do not change, but the magnitudes significantly increase after protonation. In the structure, the better conjugation of the protonated *trans* diradical and two reduced CCNC and CCCN torsion angles of the protonated *cis* one make for a more efficient spin transport, promoting the spin polarization, thus leading to larger spin couplings. In terms of mechanism, the proton-induced magnetic enhancement should be attributed to strong participation of the coupler BA through its lowest unoccupied molecular orbital (LUMO) with a lower energy level after protonation, and the small HOMO–LUMO (HOMO: highest occupied molecular orbital) gap of the coupler BA through protonation is crucial in explaining such remarkable spin-coupling enhancement. Furthermore, different linking modes of the radical groups to the couplers are also considered to confirm our conclusions. In addition, we also make a comparison of the magnetic coupling strengths among their isoelectronic analogues of BA-, AB- and stilbene-bridged nitroxide diradicals before or after protonation, and find a linear correlation among them. It should be noted that the magnetic behaviors of all these diradicals obey the spin alternation rule and singly occupied molecular orbital (SOMO) effect. This work provides helpful information for the rational design of promising magnetic molecular switches.

Received 16th August 2022
Accepted 27th October 2022

DOI: 10.1039/d2ra05115j

rsc.li/rsc-advances

1. Introduction

Schiff bases and their metal complexes have attracted intensive attention from experimentalists as well as theoreticians because of possible applications in the fields of medicine, catalysis, analytical chemistry and photochromism.[1–11] Aromatic Schiff bases are among the most investigated compounds due to their stability associated with optical and electrical properties.[8–19] Benzylideneaniline (BA), an aromatic Schiff base, is of major importance in chemistry and biochemistry, belonging to the family of compounds containing the –CH=N– double bond.[8–16] As a kind of significant organic optoelectronic compound, BA and its derivatives have generated considerable interest for their potential optoelectronic properties. For example, it is reported that BA and its derivatives can exhibit favorable nonlinear optical behaviors.[8] In addition, BA and its derivatives can undergo a reversible *trans*/*cis* isomerization between the stable *trans* configuration and metastable *cis* configuration upon photoexcitation.[11–15] Based on this photochromic property, Luo *et al.* investigated systematically the substitution and solvent effects on the *cis* → *trans* thermal isomerization kinetics of BA in light of theoretical calculations and NMR spectroscopy experiments.[14] Besides, Kawatsuki and coworkers synthesized two types of polymethacrylates with BA-derivative side groups and explored their axis-selective photoreaction and photoinduced orientation depended on the photochromic behavior and the connecting direction of the BA-derivative side groups.[15] More interestingly, BA is structurally similar and isoelectronic with photochromic molecules of stilbene (the CH=CH bond) and azobenzene (the N=N bond, AB).[12] It has been established that both stilbene and AB are excellent couplers between two magnetic centers and especially the magnetic character of stilbene- or AB-bridged diradicals can change upon irradiation with appropriate wavelengths of light.[20–26] However, whether the BA-bridged diradicals could exhibit such photo-switching behaviors has not been reported heretofore. In view of this,

[a]*Department of Materials Science and Engineering, Jinzhong University, Jinzhong, 030619, People's Republic of China. E-mail: 978755183@qq.com*

[b]*School of Chemistry and Chemical Engineering, Shandong University, Jinan, 250100, People's Republic of China*

† Electronic supplementary information (ESI) available. See DOI: https://doi.org/10.1039/d2ra05115j

we select BA as the target coupler to design novel diradicals and explore their magnetic characters.

In addition to the photoinduced property, protonation is an efficient strategy to modify BA and its derivatives. The mono-protonated (protonation at the imine nitrogen) *trans*-BA has been investigated experimentally and theoretically, suggesting that protonation would restore its conjugation through removal of the lone pair of electrons on the imine nitrogen.[27,28] According to the literature,[29–34] the increased conjugation of *trans*-BA after protonation can create advantageous condition for spin transmission of the *trans*-BA-bridged diradical. That is to say, protonation may enhance the magnetic coupling of the *trans*-BA-bridged diradical. In fact, it has been demonstrated that the proton-induced magnetic regulation (including magnetic switching, enhancement or weakening, *etc.*) in the organic systems is easy to accomplish and likely to find promising applications in magnetic data storage.[26,35–39] Sandberg *et al.* observed the generation of ground state triplet (T) diradicals by means of the proton-induced intramolecular electron transfer from the donor unit to the cross-conjugated acceptor for the species with a closed-shell (CS) ground state.[36] Moreover, Yamashita and coworkers synthesized a solvatochromic phenol-linked imidazole derivative and revealed that this molecule has switchable spin states between CS singlet and broken-symmetry (BS) open-shell singlet state *via* proton tautomerism.[38] In particular, we noticed that the magnetic enhancement occurs for several couples of the AB-bridged diradicals after protonation at the azo unit.[26]

Inspired by these, herein we theoretically design the *trans*-/*cis*-BA-based diradicals in which two nitroxide radicals are linked to the *para* positions (the pp series) of the two phenylene units with respect to the –CH=N– unit, and the imine nitrogen could undergo single protonation to convert to its protonated counterpart (–CH=NH$^+$–). As evidenced at the B3LYP level of theory, the calculated results suggest that the antiferromagnetic (AFM) couplings of two unprotonated pp-type diradicals are relatively large regardless of the *trans* or *cis* configurations, attributed to the good mediating ability of the highest occupied molecular orbital (HOMO) of the coupler BA. Moreover, the dominating finding is that protonation can considerably enhance the AFM couplings of two pp-type diradicals. That is, the signs of their magnetic exchange coupling constants J do not change, but the magnitudes significantly increase after protonation no matter for the *trans* or *cis* forms. On the one hand, the changes in geometric structures of diradicals are responsible for such noticeable magnetic enhancement induced by protonation. The better conjugation of the protonated *trans* diradical and two reduced CCNC and CCCN torsion angles of the protonated *cis* one make for a more efficient spin transport, promoting the spin polarization and then leading to larger magnetic couplings. On the other hand, the proton-induced magnetic enhancement should be attributed to strong participation of the coupler BA through its lowest unoccupied molecular orbital (LUMO) with a lower energy level after protonation. Furthermore, the small HOMO–LUMO gap of the coupler BA through protonation is significant to assist in the explanation of such remarkable spin-coupling enhancement. In addition, different connection modes of two radical groups to the coupler are also considered to further verify the conclusion of protonation-enhanced magnetic coupling. Interestingly, it is observed that changing the connection modes of two radical groups can not only adjust the magnitude of J but also modifies the sign of J from AFM to ferromagnetism (FM), suggesting a possibility of the connecting-mode-independent magnetic switching. Besides, we also make a comparison of the magnetic coupling strengths among the isoelectronic analogues of BA-, AB- and stilbene-bridged nitroxide diradicals before or after protonation, and find a linear correlation among them. Finally, it is worth mentioning that the magnetic behaviors (including FM and AFM) of all these diradicals can be predicted by means of the spin alternation rule[40,41] and singly occupied molecular orbital (SOMO) effect.[42] This work may broaden the landscape for the rational design of the BA-bridged modulators or switches and further it is shown that protonation is an effective method to enhance magnetic coupling.

We explain the terms of spin transport, spin polarization and spin alternation rule mentioned above as follows. For a diradical system, spin transport refers to the distribution of unpaired electrons in the spin center along with the π-conjugated coupling unit and spin polarization results from different interactions between unpaired electrons in partially occupied orbitals and paired electrons. The spin alternation rule states that the adjacent atomic center in a π-conjugated diradical prefers opposite spins, in other words, alternating α and β spins.

2. Design scheme and computational details

In general, both the coupler and radical groups are essential for a diradical. In this context, we choose the relatively stable nitroxide (NO) radical as magnetic centers and attach them to the *trans* and *cis* forms of BA at the *para* positions, respectively, denoted as NO-^{t}(C=N)-pp (*t*: the *trans* form) and NO-^{c}(C=N)-pp (*c*: the *cis* form), as depicted in Scheme 1. After protonation, NO-^{t}(C=N)-pp and NO-^{c}(C=N)-pp convert to NO-^{t}(C=NH$^+$)-pp and NO-^{c}(C=NH$^+$)-pp, respectively. In addition, to further confirm the protonation effect on the magnetic couplings and meanwhile examine the influence on magnetic characters due to different linking modes, two NO radical groups are linked to the couplers BA/BAH$^+$ in the *trans* and *cis* forms at the *meta*/*para* (mp) or *meta*/*meta* (mm) sites, denoted as NO-^{t}(C=N)-mp/NO-^{t}(C=NH$^+$)-mp, NO-^{c}(C=N)-mp/NO-^{c}(C=NH$^+$)-mp, NO-^{t}(C=N)-mm/NO-^{t}(C=NH$^+$)-mm and NO-^{c}(C=N)-mm/NO-^{c}(C=NH$^+$)-mm, respectively, as illustrated in Scheme 1. As isoelectronic analogues of the BA/BAH$^+$-bridged NO diradicals, the AB/ABH$^+$- and stilbene-based NO diradicals of three series in the *trans* and *cis* forms are also listed in Scheme S1,† denoted as NO-^{t}(N=N)-pp/NO-^{t}(N=NH$^+$)-pp, NO-^{c}(N=N)-pp/NO-^{c}(N=NH$^+$)-pp, NO-^{t}(N=N)-mp/NO-^{t}(N=NH$^+$)-mp, NO-^{c}(N=N)-mp/NO-^{c}(N=NH$^+$)-mp, NO-^{t}(N=N)-mm/NO-^{t}(N=NH$^+$)-mm, NO-^{c}(N=N)-mm/NO-^{c}(N=NH$^+$)-mm, NO-^{t}(C=C)-pp, NO-^{c}(C=C)-pp, NO-^{t}(C=C)-mp, NO-^{c}(C=C)-mp, NO-^{t}(C=C)-mm and NO-^{c}(C=

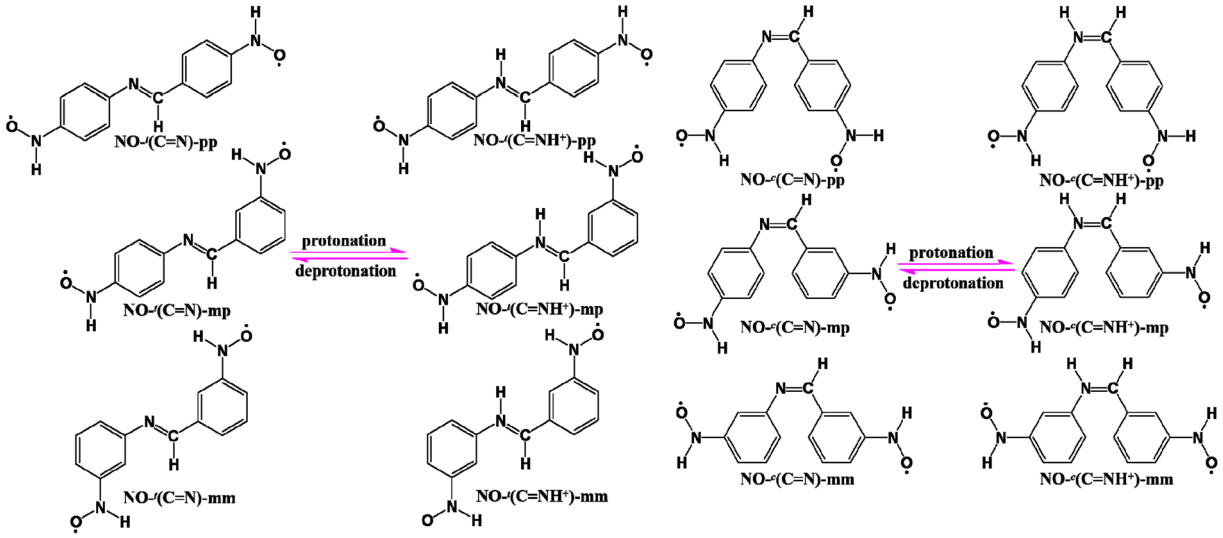

Scheme 1 Schematic diagram of the unprotonated and protonated structures for the *trans*- and *cis*-forms of BA-based diradicals with two nitroxide (NO) radical groups at the *para*-/*para*- (pp), *meta*-/*para*- (mp) or *meta*-/*meta*- (mm) sites.

C)-mm, respectively. It should be pointed out that the stilbene-bridged NO diradicals have no protonated counterparts and the following relevant data related to the *trans*/*cis*-AB/ABH$^+$-bridged NO diradicals are all from ref. 26.

The Heisenberg spin Hamitonian can be utilized to express the magnetic exchange interaction between two magnetic centers 1 and 2: $\hat{H} = -2J\ \hat{S}_1 \times \hat{S}_2$, where $\hat{S}_1$ and $\hat{S}_2$ are the respective spin angular momentum operators, with J being the magnetic exchange coupling constant. The positive and negative sign of J is a representative of FM and AFM interactions, respectively. It has been demonstrated that the electronic states of the singlet and triplet would be the eigenstates of the Heisenberg Hamitonian, and their corresponding energy eigenvalues are $E(S = 0; S) = 3J/2$ and $E(S = 1; T) = -J/2$. Therefore, for a diradical system, J can be written as: $E(S = 1) - E(S = 0) = -2J$. That is to say, the J value of a diradical can be evaluated by simply determining the exact singlet and triplet energy values. The unrestricted Hartree–Fock (UHF) methodology based on a single determinantal wave function can be adopted to reasonably describe the triplet geometry, but it is not capable of describing the singlet of a diradical due to the introduction of spin contamination, yielding an unreliable J accordingly.[43,44] The multiconfigurational approach and self-consistent field calculations are suitable to estimate J, but these methods are resource intensive and not practical for large molecules.[45,46] In this study, we employ the broken-symmetry formalism proposed by Noodleman[47,48] in a density functional theory (DFT) framework to evaluate J, which is an alternative approach to properly describe the singlet of a diradical with a lower computational cost. Based on this, the expression of J was developed and pointed out by Yamaguchi and co-workers[49,50] with the use of spin-projected methods, given as: $J = (E_{BS} - E_T)/(\langle S^2\rangle_T - \langle S^2\rangle_{BS})$, where E_{BS}, E_T, $\langle S^2\rangle_{BS}$ and $\langle S^2\rangle_T$ refer to the energies and average spin square values of the BS and T states, respectively. This formula is considered as the most applicable and popular one for estimating J for the diradical systems.

In principle, the DFT-based methods tend to overestimate J, but the B3LYP functional has been widely accepted to evaluate J of several organic diradical systems.[31,51,52] Thus the molecular geometric optimizations and frequency analyses as well as energy calculations of the CS, BS and T states of all these studied diradicals were performed at the (U)B3LYP/6-311++G(d,p) level. To confirm the rationality of some calculated results, the single-point calculations are done using CASSCF(4,6) level with the 6-311++G(d,p) basis set based on the above optimized structures. Besides, a more modern M06-2X function with the 6-311++G(d,p) basis set was adopted to further verify the accuracy of some computational results. Here, we select an adequately large 6-311++G(d,p) basis set with more polarization and diffuse functions to obtain more reliable J of the studied diradicals. All of these DFT calculations were carried out by using the suit of Gaussian 09 program.[53]

3. Results and discussion

3.1 Magnetic coupling characteristics

Depending on different connection ways among the coupler (BA or BAH$^+$) and two NO radical groups, we discuss the magnetic coupling characteristics of three kinds of diradicals categorized as the pp, mp and mm series. The calculated absolute J ($|J|$) in the *trans* and *cis* forms are shown in Fig. 1, which are in an order pp > mp > mm for the unprotonated or protonated diradicals. More detailed data including their energies of the CS, BS and T states, $\langle S^2\rangle$ values associated with J values at the (U)B3LYP/6-311++G(d,p) level are gathered in Table S1.† Regardless of the unprotonated or protonated diradicals, it is observed that the pp- and mm-type ones are all in favor of an AFM interaction, while the mp-type ones are in support of a FM coupling. The above analyses reveal that change of the connecting modes of the radical group can affect not only the magnetic magnitudes but also the magnetic behaviors of the studied diradicals. Besides, it is very interesting to note that the signs of J do not

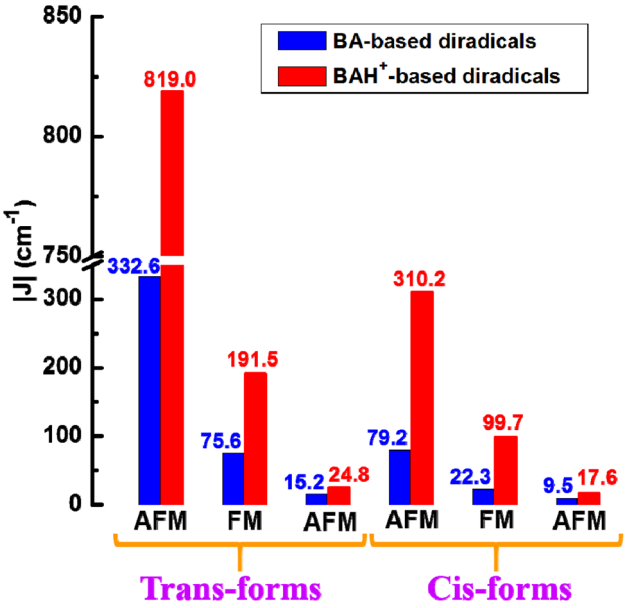

Fig. 1 Magnetic coupling constants |*J*| of unprotonated (blue) and protonated (red) diradicals including the *trans*-diradicals NO-^{t}(C=N)-pp/NO-^{t}(C=NH^{+})-pp, NO-^{t}(C=N)-mp/NO-^{t}(C=NH^{+})-mp and NO-^{t}(C=N)-mm/NO-^{t}(C=NH^{+})-mm and the corresponding *cis*-diradicals NO-^{c}(C=N)-pp/NO-^{c}(C=NH^{+})-pp, NO-^{c}(C=N)-mp/NO-^{c}(C=NH^{+})-mp and NO-^{c}(C=N)-mm/NO-^{c}(C=NH^{+})-mm from left to right in order.

change before and after protonation, but the magnitudes of the protonated diradicals noticeably increase in comparison with those of the unprotonated ones especially for the pp series (Fig. 1). Specifically, through protonation the *J* value of NO-^{t}(C=N)-pp increases from −332.6 to −819.0 cm^{-1} (NO-^{t}(C=NH^{+})-pp). For NO-^{c}(C=N)-pp, the magnitude of magnetic enhancement induced by protonation is also obvious, being about 231 cm^{-1}. In particular, there is a linear correlation between |*J*| of three types of the BA-bridged diradicals before and after protonation as shown in Fig. 2a. It is observed that the magnitudes of |*J*| for the protonated diradicals are about 2.43 times larger than that with the unprotonated ones. In Table S2,† the *J* values estimated at the UM06-2X/6-311++G(d,p) level are also presented for the purpose of comparison, including diradicals NO-^{t}(C=N)-pp, NO-^{t}(C=NH^{+})-pp, NO-^{t}(C=N)-mp, NO-^{t}(C=N)-mp, NO-^{t}(C=N)-mm and NO-^{t}(C=N)-mm. The results show that the calculated *J* are relatively accurate by employing B3LYP and M06-2X functions, and after protonation the magnetic enhancement occurs in these three couples of diradical molecules. The B3LYP functional tend to overestimate *J*, compared with the M06-2X function. The single-point calculations of NO-^{t}(C=N)-pp, NO-^{t}(C=NH^{+})-pp, NO-^{t}(C=N)-mp, NO-^{t}(C=N)-mp, NO-^{t}(C=N)-mm and NO-^{t}(C=N)-mm are also done using CASSCF(4,6) level with the 6-311++G(d,p) basis set. In Table S3,† their related singlet–triplet energy differences are obtained, corresponding to −208.2, −554.2, 50.6, 121.9, −8.6 and −14.6 cm^{-1}, respectively, demonstrating the feasibility by

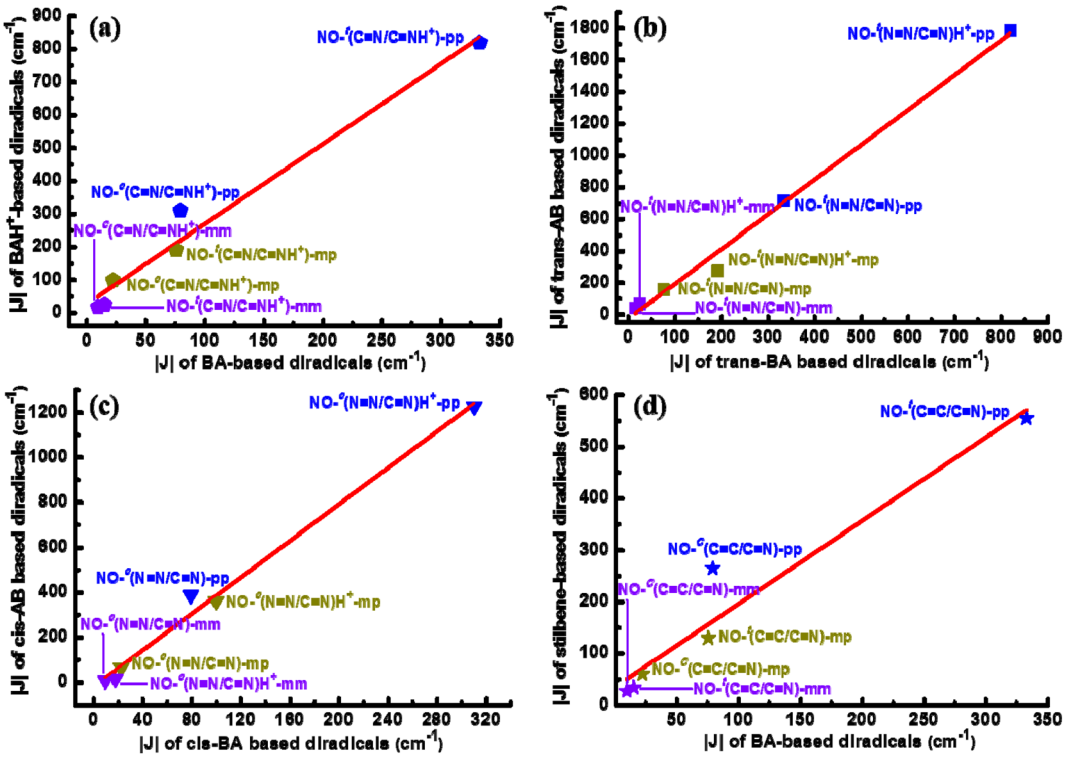

Fig. 2 Linear correlations among the computational |*J*| of the isoelectronic analogues of the NO diradicals. (a) BA *versus* BAH^{+} in the *trans* and *cis* forms, (b) *trans*-BA *versus trans*-AB before and after protonation, (c) *cis*-BA *versus cis*-AB before and after protonation, (d) BA *versus* stilbene in the *trans* and *cis* forms.

adopting (U)B3LYP/6-311++G(d,p) level again. Furthermore, to fully reflect the protonation-induced magnetic increase and compare the spin-coupling-mediating ability of the coupler BA and its isoelectronic analogues AB and stilbene, Fig. 2 also displays the linear correlations among the computational $|J|$ for the BA-, AB- and stilbene-bridged NO diradicals of the pp, mp and mm series. It can been seen that single protonation of –CH═N– or –N═N– unit can promote the magnetic couplings of the BA- or AB-bridged diradicals indeed. Moreover, we notice that for the *trans* diradicals the magnitude of the magnetic coupling strength of the AB-bridged ones is 2.19 times that of the BA-bridged ones before or after protonation (Fig. 2b), while the multiple increases to 4.06 for the *cis* forms (Fig. 2c). A comparison among the magnitudes of $|J|$ for the BA-bridged verse stilbene-bridged diradicals in the *trans* and *cis* forms indicates that the slope is about 1.61 (Fig. 2d). These observations imply that the coupler BA possesses a relatively weaker spin-coupling-mediating ability compared with AB and stilbene. Whereas, we notice that the degree of planarity of the BA-bridged diradicals can highly enhance upon protonation especially for the *trans* forms, thus facilitating the spin couplings, in contrast to the AB-bridged ones. The structural properties discussed below are responsible to all these observed phenomena including the proton-induced magnetic enhancement and the magnetic differences of diradicals with different connecting modes of the radical groups or different coupling units. It should be noted that the pp-type diradicals are mainly used as examples in the following discussion.

It is worth mentioning that a representative *trans*-AB-bridged diradical has been successfully synthesized experimentally, in which two nitronyl nitroxide radicals as the spin centers are attached to the *meta*/*para* sites of *trans*-AB.[22] Magnetic susceptibility measurements revealed that the two radical centers coupled in a ferromagnetic way, which is consistent with the sign of J of the mp series of *trans*-AB or *trans*-BA-bridged diradicals studied in this paper. Besides, Iwamura *et al.*[20] explored the magnetic coupling between two sterically protected phenoxyl radicals through the *cis*- and *trans*-stilbene chromophores by means of their EPR fine structures and concluded that m,m′-isomers of the *trans* and *cis* forms exhibit antiferromagnetic couplings. The singlet–triplet energy gaps ($\Delta E_{S-T} = 2J$) were estimated to be $0 > \Delta E_{S-T} > -35$ cal mol^{-1} (1 cal = 4.184 J) for both geometrical isomers. The reported magnitudes and signs of J are in harmony with the mm series of *cis*- and *trans*-stilbene-bridged diradicals studied in this paper. The above results demonstrate the rationality of the calculations using B3LYP function.

3.2 Molecular structures

As known, the magnetic coupling strengths are directly relevant to the structural properties of diradicals and their $|J|$ drastically decrease with the increase in the dihedral angle.[29–34] The geometric optimizations in Fig. 3 suggest that the coupler BA and two NO radical groups of the unprotonated *trans*- or *cis*-diradicals are nonplanar within three series. For the *trans* diradicals NO-^{t}(C═N)-pp, NO-^{t}(C═N)-mp and NO-^{t}(C═N)-mm, the structural distortions can be attributed to the repulsion between two hydrogen atoms from the bridge –HC═N– unit and phenylene ring. While the *cis* diradicals NO-^{c}(C═N)-pp, NO-^{c}(C═N)-mp and NO-^{c}(C═N)-mm adopt the bent conformations with the radicalized phenylene (HON-phenylene) twisted out of the plane of the –HC═N– unit. After protonation, the C–N bond length of the bridge –HC═N– unit for the *trans* diradicals is stretched and then the repulsion between two hydrogen atoms from the bridge –HC═N– unit and phenylene ring is largely weakened. As a result, the CCNC torsional angle (ϕ_1) between the HON-phenylene radical moiety and bridge –HC═N– unit within the protonated *trans* diradicals decreases for NO-^{t}(C═NH$^+$)-mm or even reduces to near zero or zero for NO-^{t}(C═NH$^+$)-mp and

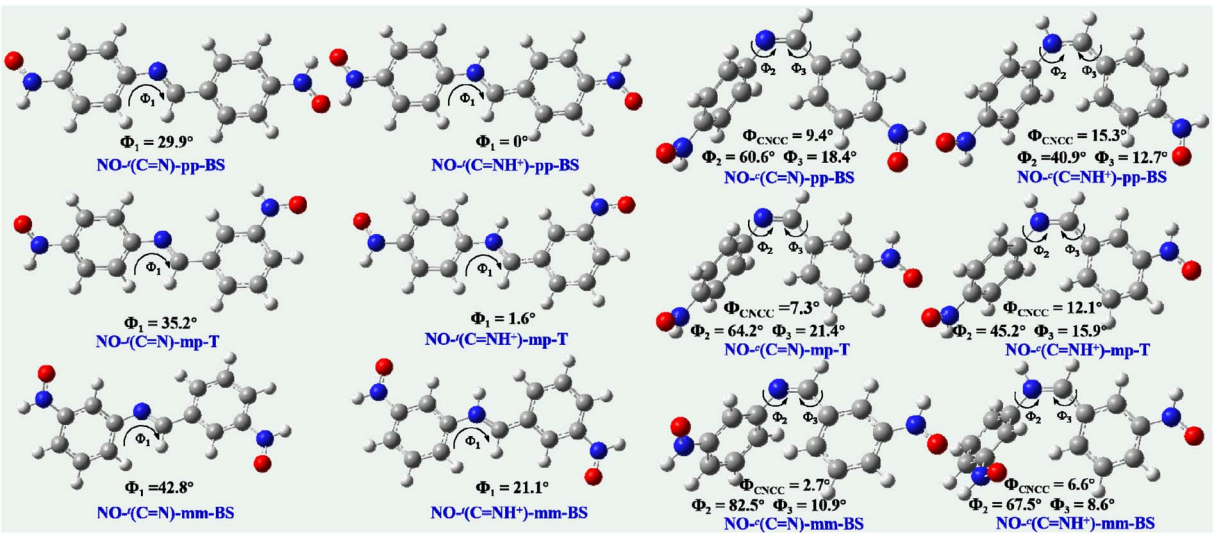

Fig. 3 Optimized geometries for the ground states of the BA-based NO diradicals of pp, mp and mm series at the (U)B3LYP/6-311++G(d,p) level, including CCNC (ϕ_1) dihedral angles for *trans*-BA-bridged diradicals, associated with CNCC (ϕ_{CNCC}), CCNC (ϕ_2) and CCCN (ϕ_3) dihedral angles for *cis*-BA-bridged ones.

NO-^{t}(C=NH$^+$)-pp (see Fig. 3), providing a beneficial condition for spin transport and then facilitating the magnetic interactions. As demonstrated, the torsional angle ϕ_1 of NO-^{t}(N=N)-pp decreases from 29.9° to 0° through protonation, leading to a larger $|J|$ value. With regard to the *cis* diradicals, after protonation the CNCC dihedral angle between two radicalized phenylene and bridge –HC=N– unit (ϕ_{CNCC}) increases, but the CCNC and CCCN torsional angles (ϕ_2 and ϕ_3) decrease (Fig. 3), facilitating the spin polarization and enhancing the spin coupling accordingly. As evidenced, after protonation the dihedral angle ϕ_{CNCC} of NO-^{c}(C=N)-pp increases from 9.4° to 15.3°, whereas the torsional angles ϕ_2 and ϕ_3 decrease from 60.6° to 40.9° and 18.4° to 12.7°, respectively. Consequently, the better conjugation of NO-^{c}(C=NH$^+$)-pp gives rise to a larger $|J|$ value compared with that of NO-^{c}(C=N)-pp. Besides, no matter for the unprotonated or protonated diradicals, we observe that the magnetic couplings of the pp, mp and mm-type ones significantly decrease in order with the increasing of the torsional angle ϕ_1 in the *trans* forms or ϕ_2 and ϕ_3 in the *cis* forms. As proved, the torsional angle ϕ_1 of NO-^{t}(C=N)-pp, NO-^{t}(C=N)-mp and NO-^{t}(C=N)-mm is 29.9°, 35.2° and 42.8° in order, and the corresponding $|J|$ are 332.6, 75.6 and 15.2 cm^{-1}, respectively.

As for isoelectronic analogues of BA/BAH$^+$, AB/ABH$^+$ and stilbene-bridged NO diradicals in the *trans* or *cis* forms in three series, the order of their magnetic magnitudes is NO–(N=N) > NO–(C=C) > NO–(C=N) or NO–(N=NH$^+$) > NO–(C=NH$^+$). Their magnetic differences in the *trans* forms are mainly due to different bond lengths of the connecting bond linking the coupler and radical group and the shorter connecting bonds of the AB/ABH$^+$-bridged diradicals provide a more facile means of magnetic interaction, while the longer ones create a disadvantage condition for magnetic coupling.[51] As evidenced, the connecting bonds of NO-^{t}(N=N)-pp, NO-^{t}(C=C)-pp and NO-^{t}(C=N)-pp are 1.382, 1.385 and 1.389 Å in order (see Fig. S1†), and their corresponding $|J|$ are 716.4, 555.4 and 332.6 cm^{-1}, respectively, presenting a negative correlation. Of course, the nonplanar structure of NO-^{t}(C=N)-pp is also an important factor for its small $|J|$. Similarly, the connecting bonds of NO-^{t}((N=NH$^+$))-pp and NO–^{t}(C=NH$^+$)-pp are 1.370 and 1.381 Å, and the corresponding $|J|$ are 1787.1 and 819.0 cm^{-1}, respectively. For the *cis* forms, their magnetic differences could be attributed to the conjugation degree and the better conjugation of the AB/ABH$^+$ or stilbene-bridged diradicals generate stronger spin coupling, whereas the worse conjugation of the BA/BAH$^+$-bridged ones produce weaker spin interactions. For example, the torsional angles of NO-^{c}(N=N)-pp (ϕ_4), NO-^{c}(C=C)-pp (ϕ_6) and NO-^{c}(C=N)-pp (ϕ_2) are 39.8°, 29.3° and 60.6° in order, and their corresponding $|J|$ are 388.1, 264.9 and 79.2 cm^{-1}, respectively. Analogously, the torsional angles of NO-^{c}(N=NH$^+$)-pp (ϕ_4) and NO-^{c}(C=NH$^+$)-pp (ϕ_2) are 2.2° and 40.9°, and the corresponding $|J|$ are 1227.9 and 310.2 cm^{-1}, respectively. The detailed data of structural properties for all these studied diradicals are shown in Fig. S1.†

3.3 Spin polarization

Except for the molecular structure, spin polarization is exceedingly instrumental in elucidating the magnetic magnitudes of π-conjugated diradicals.[26,51] The magnetic enhancements induced by protonation can be quantitatively interpreted with the help of spin polarization from the NO radical group to the coupler BAH$^+$ on the basis of the Mulliken atomic spin density distributions. Furthermore, the differences in $|J|$ for these BA/BAH$^+$-based diradicals in three series are also attributed to different atomic spin density distributions due to different linking sites of the NO groups. As presented in Fig. 4, it is evident that the average spin density delocalization into the coupler *trans*- or *cis*-BA for the protonated diradicals is larger than that of the corresponding unprotonated ones for the pp, mp and mm series. Specifically, 17.4%, 13.7% and 12.3% of spin densities are delocalized to the *trans*-BA coupler for the unprotonated diradicals NO-^{t}(C=N)-pp, NO-^{t}(C=N)-mp and NO-^{t}(C=N)-mm, while spin polarization is prominently increased to 26.8%, 17.4% and 12.8% in the case of the protonated ones NO-^{t}(C=NH$^+$)-pp, NO-^{t}(C=NH$^+$)-mp and NO-^{t}(C=NH$^+$)-mm. As a result, the larger spin polarization of these protonated diradicals strengthens the spin coupling interaction between two NO groups. Analogously, after protonation spin polarization towards the *cis*-BA coupler is enhanced from 15.4% to 23.2%, 13.5% to 16.0% and 12.6% to 13.2%, with respect to NO-^{c}(C=N)-pp, NO-^{c}(C=N)-mp and NO-^{c}(C=N)-mm, further manifesting that protonation can promote the spin polarization effect. On the whole, we can draw the following two conclusions: (1) the protonated diradicals exhibit stronger spin polarization featuring the larger $|J|$; (2) regardless of the unprotonated or protonated diradicals, it is evident that spin polarization is in an order pp > mp > mm in the *trans* and *cis* forms, accordant with their corresponding $|J|$.

Similarly, different magnetic magnitudes with respect to isoelectronic analogues of the BA/BAH$^+$, AB/ABH$^+$ and stilbene-bridged NO diradials in the *trans* or *cis* forms within three series can also be accounted for by means of the spin polarization effect. For example, the atomic spin density distributions in the NO radical groups are 82.6%, 80.7% and 78.6% for the *trans* diradicals of NO-^{t}(N=N)-pp, NO-^{t}(C=C)-pp and NO-^{t}(C=N)-pp (see Fig. S2†), corresponding to 716.4, 555.4 and 332.6 cm^{-1} in

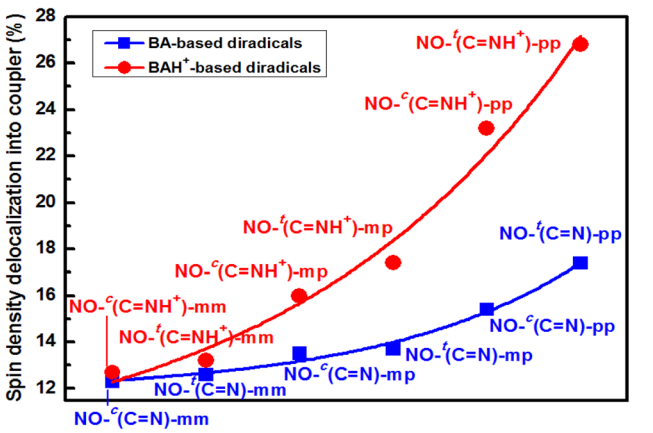

Fig. 4 Average percentages of atom spin density distributions delocalized into the coupler BA for the unprotonated and protonated NO diradicals.

order, which suggests that the largest spin polarization of NO-^{t}(N=N)-pp can strongly promote the spin coupling between two NO groups, and the relatively larger spin polarization of NO-^{t}(C=C)-pp generates a moderate magnetic interaction, while the smallest spin polarization of NO-^{t}(C=N)-pp leads to the weakest coupling interaction. With regard to NO-^{t}(N=NH^{+})-pp and NO-^{t}(C=NH^{+})-pp, 42.4% spin density is delocalized over the *trans*-ABH^{+} coupler and 26.8% spin density is delocalized over the *trans*-BAH^{+} coupler, and consequently the larger spin polarization of NO-^{t}(N=NH^{+})-pp considerably facilitates magnetic coupling compared with that of NO-^{t}(C=NH^{+})-pp. The Mulliken atomic spin density distributions of all the studied diradicals are depicted in Fig. S2.†

3.4 Mechanism of magnetic interaction

As mentioned above, the magnitude of J of the BA-based diradicals depends greatly on the coplanarity between the radical groups and bridging unit and the more extensive π-conjugation is beneficial to spin polarization for the protonated diradicals, thus promoting the spin coupling interactions. While it has been established that the good conjugation of a diradical arises from an effective molecular orbital overlap between the coupler and radical group.[26,54] Thereby it is essential to analyze the orbital properties and orbital energy level of the coupler BA and NO radical group to further clarify the protonation-induced magnetic enhancement. Interestingly, we notice that there is a good orbital matching of two SOMOs of the NO groups with the HOMO of the coupler *trans*-BA or *cis*-BA for the unprotonated diradicals, or with the LUMO of the coupler *trans*-BAH^{+} or *cis*-BAH^{+} for the protonated ones, as depicted in Fig. 5 and S3.† That is, the coupler HOMO plays a large mediating role in controlling the magnetic couplings for the unprotonated diradicals, while the coupler LUMO is more critical in determining the enhanced magnetic interactions for the protonated ones.

To quantitatively explain the proton-induced magnetic enhancement and confirm the different magnetic coupling mechanisms of the unprotonated and protonated diradicals, we further examine the orbital energy levels of the coupler and radical group. As shown in Fig. 6a, both the energies of HOMO and LUMO of the coupler *trans*-BA or *cis*-BA decrease after protonation. That is to say, introduction of a proton into the couplers *trans*-BA or *cis*-BA can decrease not only their HOMO energy levels, but also their LUMO energy levels to a large extent. Specifically, upon protonation the energies of HOMO and LUMO reduce by 4.24 and 5.02 eV for the *trans*-BA, and by 4.82 and 5.03 eV for the *cis*-BA, respectively. It has been suggested that if the orbital energies of the SOMO (HOMO) of the radical groups and HOMO of the coupler are very close, they can combine together to form a stable diradical with considerable spin–spin coupling, or *vice versa*.[54] Interestingly, we observe that the energy difference of HOMO between the *trans*-/*cis*-BA

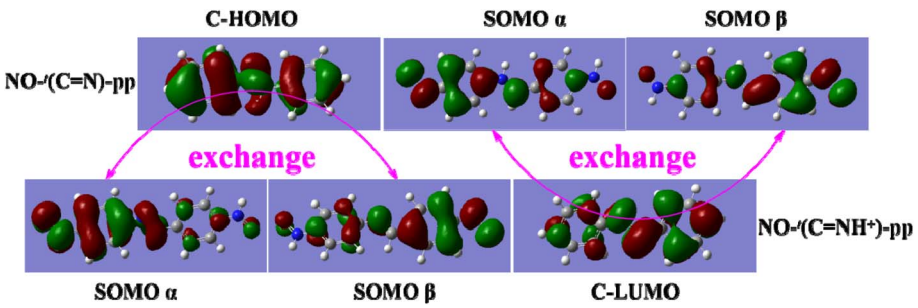

Fig. 5 Exchange couplings between two SOMOs of diradicals NO-(C=N)-pp and NO-^{t}(C=NH^{+})-pp though their corresponding couplers (C) HOMO or LUMO.

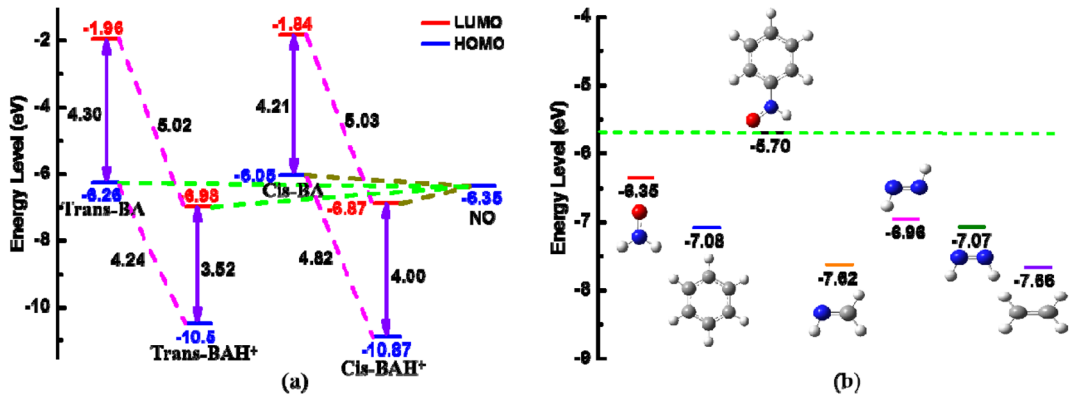

Fig. 6 (a) HOMO and LUMO energy levels of the couplers *trans*-BA, *trans*-BAH^{+}, *cis*-BA and *cis*-BAH^{+} as well as the NO group (b) HOMO energy levels for the model molecules of the bridges of the coupler BA-, AB- and stilbene saturated by hydrogen atoms and the nitroxide-phenyl radical.

coupler and NO radical group is very close, demonstrating that the coupler HOMO is critical to adjust the spin coupling of two spin sources for the unprotonated diradicals. While the energy difference of LUMO of the *trans*-/*cis*-BAH^+ coupler and HOMO of the NO radical group is much smaller, consistent well with the aforementioned opinion that the coupler LUMO plays a decisive role for the magnetic interactions for the protonated diradicals. Furthermore, we have found that small HOMO–LUMO energy gap of the protonated coupler *trans*-BAH^+ (3.52 eV) or *cis*-BAH^+ (4.00 eV) can effectively promote the magnetic coupling of diradical in contrast to that of *trans*-BA (5.02 eV) or *cis*-BA (5.03 eV).[55,56] The schematic representation of the exchange coupling interactions between two spin centers through the coupler HOMO (the unprotonated diradicals) or LUMO (the unprotonated diradicals) together with its HOMO–LUMO energy gap is collected in Fig. S4.†

To further explain different magnetic magnitudes of isoelectronic analogues of the BA, AB and stilbene-based NO diradicals, we also analyze the energy difference between the radical groups and bridging unit among them. The reason is that small energy difference of HOMO between the radical groups and bridging unit is favorable to the formation of a stable diradical, leading to a strong spin coupling. The HOMO energy levels of the model molecular segments including the HON-phenylene radical moiety and NO radical group as well as bridging units –HC═N–, –HC═CH– and –N═N– are illustrated in Fig. 6b. The calculated results reveal that larger HOMO energy differences between HON-phenylene and –HC═N– or –HC═CH– give rise to smaller magnetic interactions for the BA or stilbene-bridged diradicals compared with that of the AB-coupled ones. This observation suggests that the orbital energy difference between the radical groups and bridging unit is substantive in governing the degree of spin coupling interaction. Besides, an effective orbital matching of two SOMOs of the NO groups with the HOMO of the coupler AB and stilbene or LUMO of the coupler ABH^+ (Fig. S3†) is crucial in determining the magnetic strength as described above. It is worth pointing out that the magnetic behaviors of all the studied diradicals obey the SOMO effect (Fig. S5†) and spin alternation rule (Fig. S6†).

4. Conclusions

In summary, we theoretically design several couples of the BA-bridged nitroxide diradicals in the *trans* or *cis* forms, whose magnetic coupling constants J have significant increases after protonation of the central –CH═N– unit of the coupler BA. It is found that although the signs of their J do not change, but the magnitudes remarkably increase after protonation from −332.6 to −819.0 cm^{-1} for NO-^{t}(C═N)-pp and −79.2 to −310.2 cm^{-1} for NO-^{t}(C═N)-pp, respectively. Structurally, the better conjugation of the protonated *trans* diradical and two reduced CCNC and CCCN torsion angles (ϕ_2 and ϕ_3) of the protonated *cis* one create a more favorable condition for spin transmission, promoting the spin polarization and then leading to larger spin couplings. More importantly, the proton-induced magnetic enhancement should be attributed to strong participation of the coupler BA through its LUMO with a lower energy level after protonation, improving spin polarization from the NO radical groups to the coupler BA and facilitating the spin coupling accordingly. Moreover, small HOMO–LUMO gap of the coupler BA through protonation is crucial in explaining such remarkable spin-coupling enhancement. In addition, different linking positions of two NO radical groups to the coupler BA are also considered to further confirm the conclusion of the protonation-enhanced magnetic couplings and we observe that their absolute J ($|J|$) are in an order pp > mp > mm for the unprotonated or protonated diradicals regardless of the *trans* or *cis* forms. Furthermore, we also make a comparison of the magnetic coupling strengths among the isoelectronic analogues of BA-, AB- and stilbene-bridged nitroxide diradicals before or after protonation, and find a linear correlation among them. The spin-coupling-mediating abilities of the isoelectronic analogues are in an order AB > stilbene > BA. Besides, the magnetic behaviors of all these studied diradicals can be qualitatively predicted by means of the spin alternation rule and SOMO effect. This work would open a new prospective for the rational design of the magnetic molecular switches (Fig. 6).

Author contributions

Fengying Zhang: writing original draft, software, validation, supervision, funding acquisition. Yiwei Feng: data curation. Xinyu Song: conceptualization, software. Yuxiang Bu: conceptualization, software.

Conflicts of interest

There are no conflicts to declare.

Acknowledgements

We are thankful for financial support from the Scientific and Technological Innovation Programs of Higher Education Institutions in Shanxi (No. 2019L0889), the National Youth Natural Fund (62105131), the Scientific and Technology Key Research and Development Project of Jinzhong City (Y201027) and the Shanxi Province Collaborative Innovation Center for Light Materials Modification and Application (No. PY201817).

References

1 T. Katsuki, *Chem. Soc. Rev.*, 2004, **33**, 437–444.
2 Y. Hu, N. Goodeal, Y. Chen, A. M. Ganose, R. G. Palgrave, H. Bronstein and M. O. Blunt, *Chem. Commun.*, 2016, **52**, 9941–9944.
3 A. Naghipour and A. Fakhri, *Catal. Commun.*, 2016, **73**, 39–45.
4 J. Chai, Y. B. Wu, B. S. Yang and B. Liu, *J. Mater. Chem. C*, 2018, **6**, 4057–4064.
5 X. W. Xu, S. Q. Ma, J. H. Wu, J. T. Yang, B. B. Wang, S. Wang, Q. Li, J. Feng, S. S. You and J. Zhu, *J. Mater. Chem. A*, 2019, **7**, 15420–15431.
6 M. Maji, S. Acharya, I. Bhattacharya, A. Gupta and A. Mukherjee, *Inorg. Chem.*, 2021, **60**, 4744–4754.

7 X. Zhang, J. Z. Wu, Z. L. Qin, L. J. Qian, L. C. Liu, W. C. Zhang and R. J. Yang, *ACS Appl. Polym. Mater.*, 2022, **4**, 2604–2613.
8 C. A. van Walree, O. Franssen, A. W. Marsman, M. C. Flipseb and L. W. Jenneskens, *J. Chem. Soc., Perkin Trans. 2*, 1997, 799–807.
9 H. Neuvonen, K. Neuvonen and F. Fölöp, *J. Org. Chem.*, 2006, **71**, 3141–3148.
10 P. Bao and Z. H. Yu, *J. Comput. Chem.*, 2006, **27**, 809–824.
11 L. Óvári, Y. Luo, F. Leyssner, R. Haag, M. Wolf and P. Tegeder, *J. Chem. Phys.*, 2010, **133**, 044707.
12 A. V. Gaenko, A. Devarajan, L. Gagliardi, R. Lindh and G. Orlandi, *Theor. Chem. Acc.*, 2007, **118**, 271–279.
13 R. Mitrić, U. Werner and V. B. Koutecký, *J. Chem. Phys.*, 2008, **129**, 164118.
14 Y. Luo, M. Utecht, J. Dokić, S. Korchak, H. M. Vieth, R. Haag and P. Saalfrank, *ChemPhysChem*, 2011, **12**, 2311–2321.
15 N. Kawatsuki, H. Matsushita, T. Washio, J. Kozuki, M. Kondo, T. Sasaki and H. Ono, *Macromolecules*, 2014, **47**, 324–332.
16 L. Y. Wang, C. T. Cao and C. Z. Cao, *J. Phys. Org. Chem.*, 2016, **29**, 299–304.
17 J. M. O. Sánchez, R. Gelabert, M. Moreno and J. M. Lluch, *J. Chem. Phys.*, 2008, **129**, 214308.
18 P. P. Zhao, P. Lu, Z. Y. Zhao, S. W. Chen, X. Y. Li, C. Deng and Y. Z. Wang, *Chem. Eng. J.*, 2022, **437**, 135461.
19 L. Zhai, Y. Jiang, Y. Shi, M. Lv, Y. L. Pu, H. L. Cheng, J. Y. Zhu and K. W. Yang, *Bioorg. Chem.*, 2022, **126**, 105910.
20 T. Mitsumori, N. Koga and H. Iwamura, *J. Phys. Org. Chem.*, 1994, **7**, 43–49.
21 A. K. Pal, S. Hansda, S. N. Datta and F. Illas, *J. Phys. Chem. A*, 2013, **117**, 1773–1783.
22 K. Hamachi, K. Matsuda, T. Itoh and H. Iwamura, *Bull. Chem. Soc. Jpn.*, 1998, **71**, 2937–2943.
23 S. I. Nakatsuji, M. Fujino, S. Hasegawa, H. Akutsu, J. I. Yamada and V. S. Gurman, *J. Org. Chem.*, 2007, **72**, 2021–2029.
24 S. Shil and A. Misra, *J. Phys. Chem. A*, 2010, **114**, 2022–2027.
25 S. N. Datta, A. K. Pal, S. Hansda and I. A. Latif, *J. Phys. Chem. A*, 2012, **116**, 3304–3311.
26 F. Y. Zhang, X. Y. Song and Y. X. Bu, *J. Phys. Chem. C*, 2017, **121**, 17160–17168.
27 H. Y. Xu, K. Sohlberg and Y. Wei, *J. Mol. Struct.*, 2003, **634**, 311–314.
28 H. Bednarski, M. Domański, J. Weszka and K. Sohlberg, *J. Mol. Struct.*, 2009, **908**, 122–124.
29 M. E. Ali and S. N. Datta, *J. Phys. Chem. A*, 2006, **110**, 2776–2784.
30 I. Latif, A. Panda and S. N. Datta, *J. Phys. Chem. A*, 2009, **113**, 1595–1600.
31 M. E. Ali, V. Staemmler, F. Illas and P. M. Oppeneer, *J. Chem. Theory Comput.*, 2013, **9**, 5216–5220.
32 F. Y. Zhang, X. Y. Song and Y. X. Bu, *J. Phys. Chem. C*, 2015, **119**, 27930–27937.
33 A. Bajaj and M. E. Ali, *J. Phys. Chem. C*, 2019, **123**, 15186–15194.
34 Q. Wang, Z. L. Zhang, H. C. Huang, X. Y. Song and Y. X. Bu, *Phys. Chem. Chem. Phys.*, 2022, **24**, 3834–3843.
35 S. Nishida, Y. Morita, K. Fukui, K. Sato, D. Shiomi, T. Takui and K. Nakasuji, *Angew. Chem.*, 2005, **117**, 7443–7446.
36 M. O. Sandberg, O. Nagao, Z. Wu, M. M. Matsushita and T. Sugawara, *Chem. Commun.*, 2008, 3738–3740.
37 M. Ishida, S. Karasawa, H. Uno, F. Tani and Y. Naruta, *Angew. Chem., Int. Ed.*, 2010, **49**, 5906–5909.
38 H. Yamashita and J. Abe, *J. Phys. Chem. A*, 2014, **118**, 1430–1438.
39 Q. Wang, X. Y. Song, P. Li and Y. X. Bu, *J. Phys. Chem. C*, 2019, **123**, 10764–10776.
40 C. Trindle and S. N. Datta, *Int. J. Quantum Chem.*, 1996, **57**, 781–799.
41 C. Trindle, S. N. Datta and B. Mallik, *J. Am. Chem. Soc.*, 1997, **119**, 12947–12951.
42 W. T. Borden and E. R. Davidson, *J. Am. Chem. Soc.*, 1977, **99**, 4587–4594.
43 D. Feller, E. R. Davidson and W. T. Borden, *Isr. J. Chem.*, 1983, **23**, 105–108.
44 S. Kato, K. Morokuma, D. Feller, E. R. Davidson and W. T. Borden, *J. Am. Chem. Soc.*, 1983, **105**, 1791–1795.
45 G. Chung and D. Lee, *Chem. Phys. Lett.*, 2001, **350**, 339–344.
46 V. Polo, A. Alberola, J. Andres, J. Anthony and M. Pilkington, *Phys. Chem. Chem. Phys.*, 2008, **10**, 857–864.
47 L. Noodleman, *J. Chem. Phys.*, 1981, **74**, 5737–5743.
48 L. Noodleman and E. J. Baerends, *J. Am. Chem. Soc.*, 1984, **106**, 2316–2327.
49 K. Yamaguchi, Y. Takahara, T. Fueno and K. Nasu, *Jpn. J. Appl. Phys.*, 1987, **26**, L1362–L1364.
50 K. Yamaguchi, F. Jensen, A. Dorigo and K. N. Houk, *Chem. Phys. Lett.*, 1988, **149**, 537–542.
51 D. Cho, K. C. Ko and J. Y. Lee, *J. Phys. Chem. A*, 2014, **118**, 5112–5121.
52 D. Cho, K. C. Ko and J. Y. Lee, *Int. J. Quantum Chem.*, 2016, **116**, 578–597.
53 M. J. Frisch, *et al.*, *Gaussian 09, Revision B.01*, Gaussian, Inc., Wallingford, CT, 2009.
54 Y. W. Feng, F. Y. Zhang, X. Y. Song and Y. X. Bu, *Phys. Chem. Chem. Phys.*, 2017, **19**, 5932–5943.
55 S. Shil, M. Roy and A. Misra, *RSC Adv.*, 2015, **5**, 105574–105582.
56 F. Y. Zhang, Q. Luo, X. F. Song, X. Y. Song and Y. X. Bu, *Int. J. Quantum Chem.*, 2018, **118**, e25693.